Mechanical properties of Al/a-C nanocomposite thin films synthesized using a plasma focus device

Z. A. Umar[a)b)], R. S. Rawat[a)], R. Ahmad[c)†], A. K. Kumar[d)], Y. Wang[a)], T. Hussain[c)], Z. Chen[d)], L. Shen[e)], and Z. Zhang[e)]

[a)] *NSSE, National Institute of Education, Nanyang Technological University, Singapore* 637616, *Singapore*
[b)] *Department of Physics, GC University,* 54000 *Lahore, Pakistan*
[c)] *Center for Advanced Studies in Physics (CASP), GC University,* 54000 *Lahore, Pakistan*
[d)] *School of Materials Science and Engineering, Nanyang Technological University, Nanyang Avenue, Singapore* 639798, *Singapore*
[e)] *Institute of Materials Research and Engineering, A*STAR (Agency for Science, Technology and Research), 3 Research Link, Singapore* 117602, *Singapore*

(Received 4 February 2013; revised manuscript received 20 May 2013; published online 10 December 2013)

The Al/a-C nanocomposite thin films are synthesized on Si substrates using a dense plasma focus device with aluminum fitted anode and operating with CH_4/Ar admixture. X-ray diffractometer results confirm the formation of metallic crystalline Al phases using different numbers of focus shots. Raman analyses show the formation of D and G peaks for all thin film samples, confirming the presence of a-C in the nanocomposite thin films. The formation of Al/a-C nanocomposite thin films is further confirmed using X-ray photoelectron spectroscopy analysis. The scanning electron microscope results show that the deposited thin films consist of nanoparticles and their agglomerates. The sizes of th agglomerates increase with increasing numbers of focus deposition shots. The nanoindentation results show the variations in hardness and elastic modulus values of nanocomposite thin film with increasing the number of focus shots. Maximum values of hardness and elastic modulus of the composite thin film prepared using 20 focus shots are found to be about 10.7 GPa and 189.2 GPa, respectively.

Keywords: dense plasma focus, X-ray photoelectron spectroscopy, field emission scanning electron microscope, elastic modulus

PACS: 52.59.Hq, 79.60.−i, 68.37.Vj, 62.20.de **DOI:** 10.1088/1674-1056/23/2/025204

1. Introduction

Amorphous carbon (short as a-C) films are attractive due to their extraordinary properties, such as high hardness, wear resistance, chemical resistance, and good tribological properties.[1–3] The a-C thin films are generally hard (about 18 GPa–80 GPa) but brittle.[4] Metal/amorphous carbon (Me/a-C) thin films improve the toughness of the thin films,[5] with moderately high hardness and, therefore, are important engineering materials for surface protection.[4] A lot of work has been done previously on Me/a-C or Me/DLC thin films using different techniques at room temperature, such as sputter deposition,[6,7] plasma assisted chemical vapor deposition (CVD),[8] and vacuum arc deposition.[9,10]

Aluminum with a silvery appearance is an attractive metal because it is soft, durable, lightweight, and ductile. Its properties, such as high resistance to corrosion on surfaces exposed to the atmosphere, good electrical and thermal conductivities and high reflectivity to both heat and light make it more attractive. Tay *et al.*[11] found that the hardness of the DLC thin films drastically reduced to 40% when doped with 10% Al. This is attributed to reduction in sp^3 hybridization with incorporation of Al in DLC. The incorporation of metal into a-C film reduces stress in the film, which leads to decrease in sp^3 content. The nanocomposite Al–C and Al/a-C:H thin films have been synthesized previously using different techniques.[7,11–13] In this paper, we synthesize the Al/a-C nanocomposite thin films on silicon substrates using a dense plasma focus (DPF) device, which utilizes a pulsed high energy density plasma source and study the structural, compositional and mechanical properties of these films.

The DPF is a simple and cost-effective device that makes use of a self-generated magnetic field that compresses the plasma up to a very high density (10^{25} m^{-3} –10^{26} m^{-3}) and high temperature (l keV–2 keV) in short duration (10^{-7} s).[14] A complex mix of high energy density plasmas, accelerated energetic ions and fast moving electrons emanated from hot and dense pinched plasma column during the radial collapse phase of DPF device, which are used for various material processes, such as thin film deposition, phase change of thin films, ion implantation, and surface modification.[15–20] We report on the synthesis of Al/a-C nanocomposite thin films on silicon substrates kept at ambient temperature using DPF, which offers interesting features such as very high deposition rate and energetic deposition process.

2. Experimental setup

The Al/a-C nanocomposite thin films are synthesized on Si substrates using Mather type plasma focus device designated as United Nation University/International Center for Theoretical Physics Plasma Focus Facility (UNU/ICTP PFF). The 3.3-kJ UNU-ICTP PFF is energized by a single Maxwell (30 μF, 15 kV) fast discharge capacitor. Figure 1 shows the

†Corresponding author. E-mail: ahriaz@gcu.edu.pk

© 2014 Chinese Physical Society and IOP Publishing Ltd

schematic illustration of a plasma focus device with the setup for the Al/a-C nanocomposite thin film deposition. Details of the plasma focus device are given elsewhere.[14] Conventionally, the electrode assembly of UNU-ICTP PFF uses a hollow copper anode, which is surrounded by six cylindrical copper cathode rods in a squirrel cage fashion. For the deposition of Al/a-C nanocomposite thin films, the central hollow copper anode was replaced by an engraved copper anode with solid aluminum top that was placed as an insert at the anode tip. Charging and discharging the capacitor once is termed a one focus shot. The high voltage probe and rogowski coil signals were used for monitoring the focusing efficiency of the DPF device for optimization purposes. The presence of intense voltage peak in the voltage probe signal or a steep current dip in the current coil signal indicates the efficiency of pinch plasma column formation process, which in turn controls all associated phenomena or parameters, such as the temperature and density of pinch and decaying plasmas, energy flux of instability accelerated charge particle beams, shock waves, etc. When the device was operated with only methane as the working gas, the good focus was inconsistent, which makes the plasma focus operation non-reliable. To avoid the inconsistency of the pinching efficiency in DPF device with methane as the operating gas, we used a CH_4/Ar admixture ratio with different admixture gas filling pressures. The charging voltage was kept at 14 kV during the entire optimization and deposition process. The optimized CH_4:Ar admixture filling gas pressure was found to be about 1.5 mbar (1 bar $= 10^5$ Pa) for a CH_4/Ar admixture ratio of 3:7. So, we used the same CH_4/Ar admixture ratio of 3:7 to synthesize the Al/a-C thin films on Si substrate placed at a distance of 10 cm above the anode tip along the anode axis. The silicon wafers were cleaned in an ultrasonic bath by rinsing first in acetone, then rinsing in ethanol, and finally in de-ionized water for 10 min each. The base pressure of 3×10^{-2} mbar was achieved using a rotary vane pump.

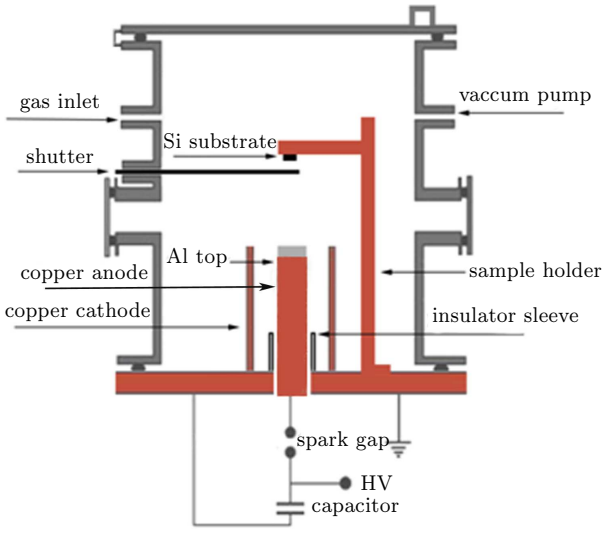


Fig. 1. (color online) Schematic diagram of DPF device.

The SIEMENS D5005 X-ray diffractometer (XRD) operated at a voltage of 40 kV and a current of 40 mA using CuK_α ($\lambda = 1.54$ Å) radiation source was used to analyze crystalline structures of deposited composite thin films. The diffraction patterns were recorded at small grazing incident angle (2°). The elemental compositions and the characteristics of bonds between Al and C were studied using thermo scientific theta probe X-ray photoelectron spectroscopy (XPS). WITEC α 300 R Confocal Raman Microscope with a laser wavelength of 488 nm was used to study the nature of a-C present in the thin film. The surface morphologies of nanocomposite thin films were studied using field emission scanning electron microscope (FESEM) [Jeol JSM-6700F], operated at a voltage of 5 kV. Nano Indenter®XP (MTS system, TN, USA) was used to study the hardness and elastic modulus of nanocomposite thin film.

3. Results and discussion

An extremely hot high energy density pinched plasma column, containing the ionic species of filling gas (such as carbon, hydrogen, and argon), is formed in front of the central electrode (anode) during the radial collapse phase of the plasma focus operation. The sausage instabilities ($m = 0$) are seen to set in hot and dense pinched/focused plasma column, which accelerates the ions (of the filling gas species) and electrons in opposite directions.[21] The hot dense pinched plasma and instability accelerated the electron beam to ablate the aluminum anode top, thereby, creating the aluminum plasma species, which also move towards the substrate surface. The qualitative description of the formation of nanocomposite Al/a-C thin film in plasma focus device operated with CH_4/Ar admixture ratio of 3:7 is as follows.

(i) The accelerated high energy ions of carbon, hydrogen, and argon of CH_4/Ar admixture ratio 3:7 bombarded the Si substrate, axially decaying high energy density plasma, and strong shock wave results in enormous and rapid increase in the temperature of the Si,[22] causing high heating and then cooling in the surface of the silicon. These ions of CH_4/Ar admixture gas are responsible for etching and cleaning the substrate surface prior to deposition.

(ii) The Al plasma, produced by the ablation of anode top, along with the background carbon plasma of the filling gas species, is deposited in the form of Al/a-C nanocomposite thin film on the silicon substrate.

(iii) The above mentioned processes happen during the first focus deposition shot, with the second one following the first. The subsequent focus deposition shot, for multiple shot depositions, will cause the processing of thin film that has already been deposited in previous shots by a complex mix of energetic ion beam, hot decaying plasma and shock wave followed by the deposition of the next layer of material.

The detailed analysis of structure, composition, morphology, and mechanical properties of the deposited Al/a-C nanocomposite thin films are given below.

3.1. Structural analysis

The XRD patterns of the nanocomposite thin films synthesized using different numbers of focus deposition shots on silicon substrates placed at the distance of 10 cm above the anode tip along the anode axis (0° angular position) are shown in Fig. 2. The XRD results show the formation of very weakly crystalline Al (111) plane for 10 focus shots and the intensity of this phase increases with increasing the number of focus deposition shots. The (200) phase of Al appears only for 30 and 40 focus deposition shots. The XRD patterns do not show any peak related to aluminum carbide. Moreover, the XPS results shown in Fig. 3(b) do not show any formation of aluminum carbide in the surface of thin film, which confirms the absence of aluminum carbide phase formation in nanocomposite thin films. The increase in the intensity of Al (111) phase with the increasing of the number of focus deposition shots may be due to the increase in the thickness as well as the energetic processing of the nanocomposite thin film. The XRD spectrum of the virgin silicon substrate exhibits only (311) diffraction plane while the samples deposited with different numbers of focus deposition shots all exhibit the formation of polycrystalline Si, with additional Si diffraction peaks being observed. The accelerated energetic ions of filling gas species, the decaying high energy density pinched plasma column, and the fast moving shock wave in DPF increase the surface temperature of the silicon substrate placed down the anode stream,[23] followed by the fast cooling that may cause the formation of polycrystalline silicon on the substrate surface.

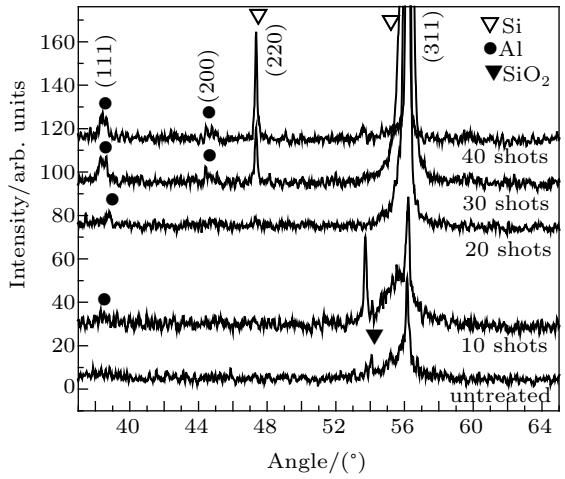


Fig. 2. XRD patterns of the thin films deposited with different numbers of focus deposition shots with a CH_4/Ar admixture ratio of 3:7.

3.2. XPS analyses

The XPS analyses of all the nanocomposite thin films deposited at 0° angular position using different numbers of focus deposition shots are performed to examine the elemental concentrations and the bondings of the elements in the surface of thin films. The different elements present in the surfaces of composite thin films, along with their atomic percentages, are given in Fig. 3(a). The analysis shows the atomic percentage of carbon increases along with the increase of the number of focus deposition shots, implying that the amount of carbon is increased in the thin film.

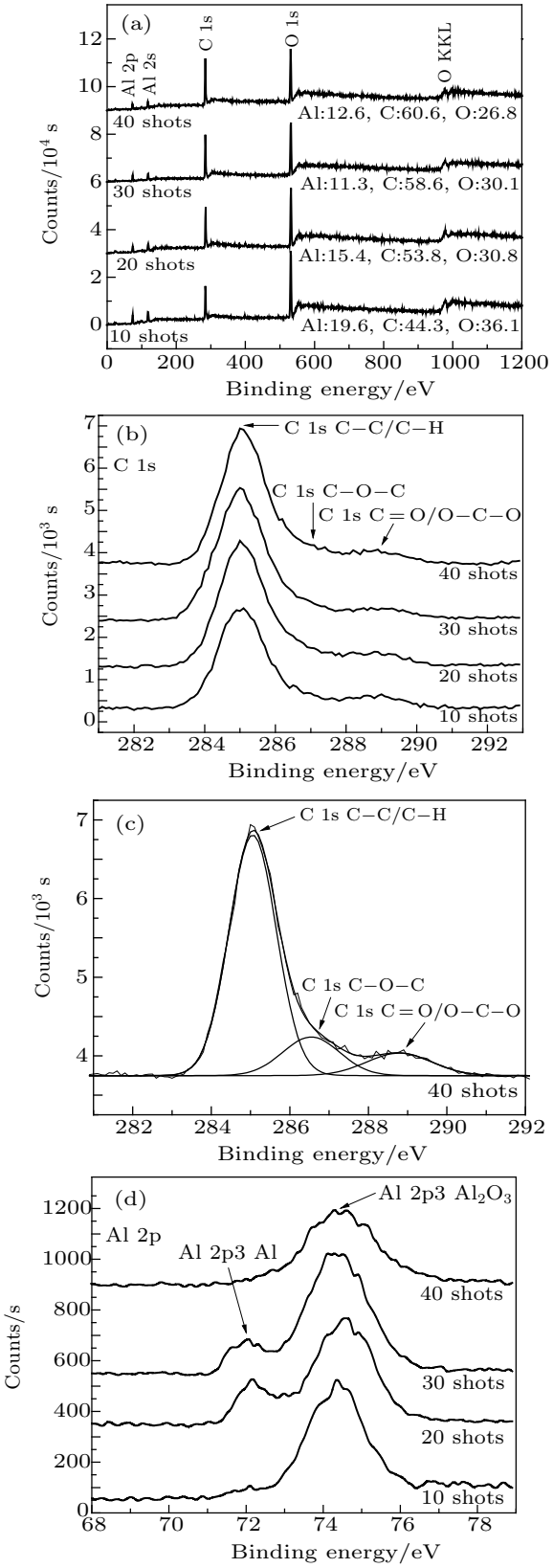


Fig. 3. XPS spectra of deposited thin films, (a) survey scan and elemental concentration with the increasing of the number of focus shots, (b) high resolution spectra of C 1s peak with different numbers of focus shots, (c) the deconvoluted C 1s peak for thin film deposited with 40 focus shots, and (d) high resolution spectra of Al 2p peak with different numbers of focus shots.

The chemical states of elements present in the surfaces of composite thin films synthesized with different numbers of focus shots can be understood by the C 1s spectra in Fig. 3(b). The XPS spectra show the presence of carbon in C–C/C–H, C–O–C, and O–C–O/C=O with their peak binding energy values of about 285, 286.7, and 288.8 eV, respectively. The C 1s spectra do not show any peak in the range from 281 eV to 283 eV for the nanocomposite thin films deposited with different numbers of focus deposition shots, indicating that carbon does not construct any bond with Al to form carbide in the surface of the thin film. The C 1s XPS spectra of one of the sample treated with 40 focus shots is deconvoluted to identify various compounds/phases that have been formed on the surface of composite thin film shown in Fig. 3(c). The deconvolution of the spectra shows the presence of C–C, C–O–C, and C=O/O–C–O on the surface of the thin film. The presence of a significant amount of oxygen on the nanocomposite thin film surface is due to the oxidation of metallic Al, which is present on the surface when the samples are exposed to atmospheric environment shown in Fig. 3(d). So, from the results obtained from XRD and XPS analyses, it is clear that Al/a-C thin film is formed on Si substrate without any Al–C bonding.

3.3. Raman analysis

The Raman analyses of the nanocomposite thin films deposited along the anode axis (0° angular position) placed at 10 cm from the anode top are shown in Fig. 4(a). The spectra show the stretching vibrations due to *D* and *G* bonds, which confirm the existence of carbon in sp^2 and sp^3 bonding configuration in composite thin films. The *D* and *G* peaks appear, respectively, at about 1366 cm^{-1} and 1600 cm^{-1}, without any considerable shift in these values for thin films deposited with different numbers of focus deposition shots. The Raman analyses also show the variations in intensity of *D* and *G* peaks with the number of focus deposition shots. The *D* and *G* peak intensities are improved for the film deposited with 40 focus shots. The pronounced intensities of *D* and *G* peaks may be attributed to the increase in surface transient temperature when the sample is treated with higher ion beam flux and energies.

The variations in the integrated *D* and *G* peak intensity ratios appearing for different thin films each as a function of the number of focus deposition shots are shown in Fig. 4(b). The I_D/I_G ratios are 1.26 and 1.27 for the films synthesized using 10 and 20 focus shots, respectively. The I_D/I_G ratios increase to the values of 1.46 and 1.38 for the films synthesized using 30 and 40 focus shots, respectively. This shows a greater amount of sp^3 content in the films deposited with 10 and 20 focus shots, since the sp^3/sp^2 ratio is inversely related to I_D/I_G ratio. The variations in ion flux and energy may be responsible for different sp^3 and sp^2 bonding content in the deposited thin films.[23] Zeb *et al.*[24] deposited diamond-like carbon films at different axial positions using the DPF device and found a similar trend of I_D/I_G value with the increasing of ion flux and energy to that in our case.

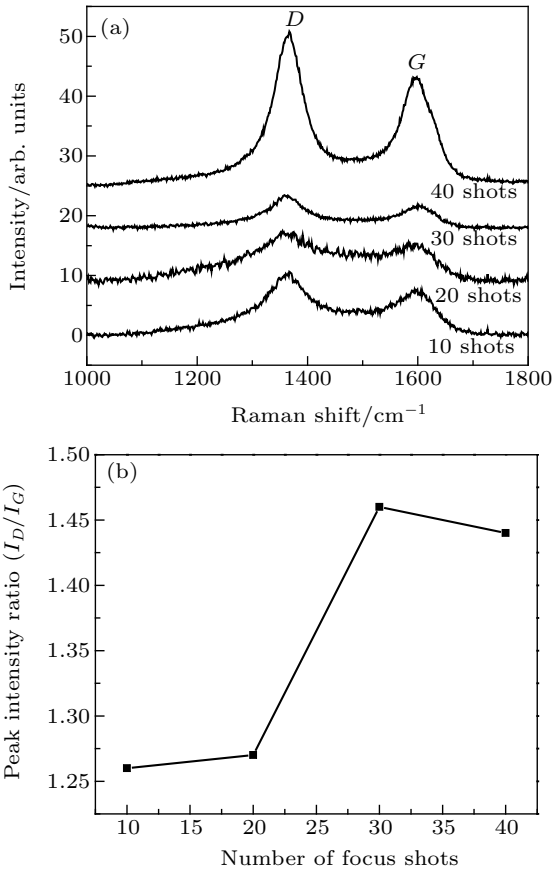


Fig. 4. Raman analyses of the thin films deposited with (a) different numbers of focus shots, with CH_4/Ar admixture ratio fixed to be 3:7, and (b) the variations in ratio between *D* and *G* peak intensities with different numbers of focus deposition shots.

3.4. Surface morphology

The surface morphologies of the nanocomposite thin films synthesized using different numbers of focus deposition shots are shown in Fig. 5. The thin films synthesized with different focus shots exhibit dense and smooth surface morphology without the presence of any cracks and voids. The scanning electron microscope results show that the surfaces of thin films deposited with different numbers of focus shots contain nanoparticles and nanoparticle agglomerates. The round shaped nanoparticles on the surfaces of thin films deposited with different numbers of focus deposition shots may indicate the presence of amorphous carbon. The size and number of agglomerates increases with the increasing number of focus deposition shots. The agglomerates form a flower-like structure for the film deposited with 40 focus deposition shots. The average size of these agglomerates for 30 and 40 focus deposition shots is more than 100 nm. The increases in the size and the number of agglomerates at higher deposition shots (30 and 40 shots) are attributed to the consequence of increases in ion energy and ion flux. The surface morphology of the thin film consists of nanoparticles and their agglomerates, which offer a large surface-to-volume ratio resulting in easy oxidation of metallic aluminium,[25,26] as observed earlier in the XPS results.

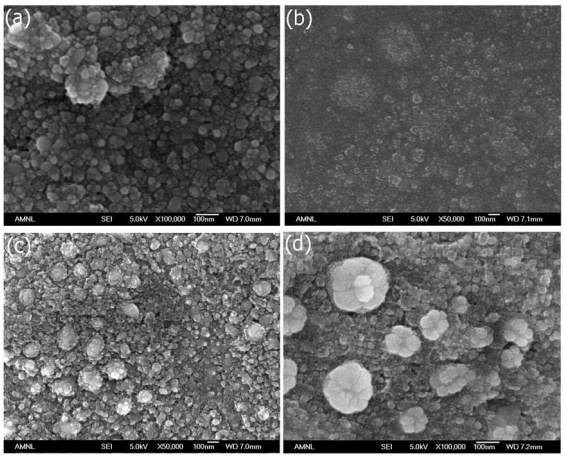


Fig. 5. Surface morphologies of the nanocomposite thin films deposited with focus shot numbers of (a) 10, (b) 20, (c), 30, and (d) 40.

3.5. Mechanical properties

The variations in hardness and elastic modulus values of the thin films synthesized with the number of focus shots are shown in Fig. 6. The mechanical properties are analyzed in terms of their chemical composition and relative sp^3 content measured by XPS and Raman spectra. The hardness and elastic modulus values of the films are taken at a depth of 100 nm to avoid the substrate effect on the measurement.

The processing of the films with different numbers of focus shots gives different compositions and structures due to the effects of ion beam flux and energy. It is evident from Table 1 that the combination of Al/C ratio and sp^3 content in the film affects the mechanical properties. The hardness and elastic modulus values of the thin films are 7.4 GPa and 155.1 GPa, respectively, which corresponds to an Al/C ratio of 0.44 and I_D/I_G value of 1.26, for 10 focus shots. The hardness and elastic modulus values for 20 focus shots are highest (10.7 GPa and 189.2 GPa). However, the sp^3 content in the film deposited with 20 focus shots with an I_D/I_G value of 1.27 is almost the same as that of the film with 10 focus shots but relatively low Al/C ratio of 0.29, which results in the increase of hardness and elastic modulus values. The film synthesized with 30 focus shots gives the lowest values of hardness and elastic modulus with I_D/I_G value of 1.46 and Al/C ratio of 0.19. The significant decrease in sp^3 content in the film results in the decrease of hardness and elastic modulus values. The hardness and elastic modulus values of the film synthesized with 40 focus shots increase again, even though the Al/C ratio is almost the same as that of the film with 30 shots. This increase in hardness and elastic modulus is due to the decrease in I_D/I_G value to 1.38 (increase in sp^3 content) in the film.

So, from the above discussion it is concluded that both Al/C ratio and sp^3 content play an important role in achieving better mechanical properties. The low Al/C ratio and high sp^3 content in the film are the key features in improving the hardness and elastic modulus values.

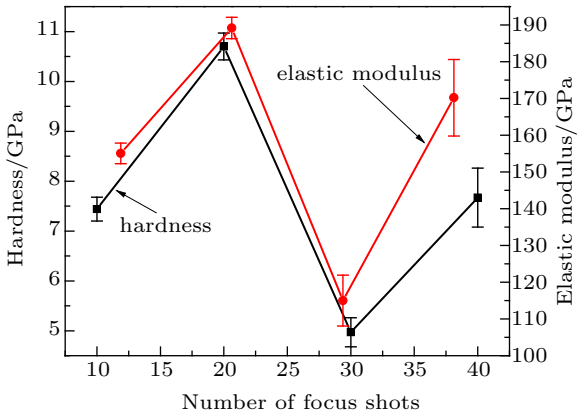


Fig. 6. (color online) Variations in hardness and elastic modulus of the thin films deposited with different numbers of focus shots.

Table 1. Elemental compositions, Al/C ratios, I_D/I_G values, hardness, and elastic modulus values of the thin films deposited with different numbers of focus shots.

Number of focus shots	Al/(at%)	C/(at%)	O/(at%)	Al/C	I_D/I_G	Hardness/GPa	Elastic modulus/GPa
10	19.6	44.3	36.1	0.44	1.26	7.4 ± 0.24	155.1 ± 2.8
20	15.4	53.8	30.8	0.29	1.27	10.7 ± 0.27	189.2 ± 2.92
30	11.3	58.6	30.1	0.19	1.46	5 ± 0.29	115 ± 6.92
40	12.6	60.6	26.8	0.21	1.38	7.7 ± 0.59	170.2 ± 10.4

4. Conclusions

The successful synthesis of Al/a-C nanocomposite thin film is achieved using a DPF device. The XRD results show crystalline phases of Al for the thin films deposited using different numbers of focus deposition shots. The Raman spectra exhibit *D* and *G* peaks due to C–C vibration modes, confirming the formation of a-C phases in composite thin films. The XPS analyses confirm the presence of metallic Al, C–C/C–H, along with oxides of aluminum and carbon on the surfaces of composite thin films. The presence of metallic Al (and absence of Al–C phase) suggests that the aluminum plasma, ablated from the aluminum top, does not react with background reactive carbon plasma. The presence of a significant amount of oxygen on the thin film surface is attributed to the oxidation of metallic Al upon exposure to atmospheric environment, which is aided by the fact that thin films are in the form of nanoparticle and nanoparticle agglomerates offering large surface-to-volume ratios. FESEM images show the smooth surface morphology consisting of nanoparticles and nanoparticle agglomerates that form nanocomposite thin films. The sizes of nano particle agglomerates increase as the number of focus deposition shots increases. The hardness and elas-

tic modulus values are found to be dependent on Al/C ratio and sp^3 content in the nanocomposite thin film. The hardness and elastic modulus values of 10.7 GPa and 189.2 GPa are achieved for thin film deposited with 20 focus deposition shots.

Acknowledgment

One of the authors (Z. A. Umar) is grateful to the HEC, Pakistan for providing financial support to conduct the reported investigation at NIE, Nanyang Technological University, Singapore.

References

[1] Robertson J 2002 *Mater. Sci. Eng. R* **37** 129
[2] Grill A 1999 *Diamond and Related Materials* **8** 428
[3] Ronkainen H, Varjus S, Koskinen J and Holmberg K 2001 *Wear* **249** 260
[4] Charitidis C A 2010 *Int. Journal of Refractory Metals & Hard Materials* **28** 51
[5] Pauleau Y, Thiery F, Barna P B, Misjak F, Kovacs A, Dub S N, Uglovand V V and Kuleshov A K 2004 *Rev. Adv. Mater. Sci.* **6** 140
[6] Pei Y T, Galvan D and De Hosson J Th M 2005 *Acta Materialia* **53** 4505
[7] Zhang G, Yan P, Wang P, Chen Y and Zhang J 2007 *J. Phys. D: Appl. Phys.* **40** 6748
[8] Pauleau Y and Thiery F 2002 *Mater. Lett.* **56** 1053
[9] Wang P, Wang X, Chen Y, Zhang G, Liu W and Zhang J 2007 *Appl. Surf. Sci.* **253** 3722
[10] Sheeja D, Tay B K, Sze J Y, Yu L J and Lau S P 2003 *Diamond and Related Materials* **12** 2032
[11] Tay B K, Cheng Y H, Ding X Z, Lau S P, Shi X, You G F and Sheeja D 2001 *Diamond and Related Materials* **10** 1082
[12] Zhou S, Wang L and Xue Q 2011 *Surface and Interface Analysis* **43** 1057
[13] Lungu C P, Ionescu V, Osiac M, Cotarlan C, Pompilian O, Lungu A M and Ciupiana V 2009 *Journal of Non-Oxide Glasses* **1** 175
[14] Lee S, Tou T Y, Moo S P, Elissa M A, Gholap A V, Kwek K H, Mulyodrono S, Smith A J, Suriyadi, Usala W and Zakaullah M 1988 *Am. J. Phys.* **56** 62
[15] Feugeas J N, Llonch E C, de González C O and Galambos G 1988 *J. Appl. Phys.* **64** 2648
[16] Kelly H, Lepone A, Marquez A, Lamas D and Oviedo C 1996 *Plasma Sources Science and Technology* **5** 704
[17] Rawat R S, Chew W M, Lee P, White T and Lee S 2003 *Surface & Coatings Technology* **173** 276
[18] Hussain T, Ahmad R, Khalid N, Umar Z A and Hussnain A 2011 *Nucl. Instrum. Methods Phys. Res. B* **269** 1951
[19] Khan I A, Jabbar S, Hussain T, Hassan M, Ahmad R, Zakaullah M and Rawat R S 2010 *Nucl. Instrum. Methods Phys. Res. B* **268** 2228
[20] Hosseinnejad M T, Ghoranneviss M, Etaati G R, Shirazi M and Ghorannevis Z 2011 *Appl. Surf. Sci.* **257** 7653
[21] Kies W, Decker G, Berntien U, Sidelnikov Yu V, Glushkov D A, Koshelev K N, Simanovskii D M and Bobashev S V 2000 *Plasma Sources Science and Technology* **9** 279
[22] Rawat R S 2012 *Nanosci. Nanotechnol. Lett.* **4** 251
[23] Murtaza G, Hussain S S, Sadiq M and Zakaullah M 2009 *Thin Solid Films* **517** 6777
[24] Zeb S, Sadiq M, Qayyum A, Murtaza G and Zakaullah M 2007 *Mater. Chem. Phys.* **103** 235
[25] Umar Z A, Rawat R S, Tan K S, Kumar A K, Ahmad R, Hussain T, Kloc C, Chen Z, Shen L and Zhang Z 2013 *Nucl. Instrum. Methods Phys. Res. B* **301** 53
[26] Ghareshabani E, Rawat R S, Sobhanian S, Verma R, Karamat S and Pan Z Y 2010 *Nucl. Instrum. Methods Phys. Res. B* **268** 2777